ASTRONOMY & ASTROPHYSICS
SUPPLEMENT SERIES

JANUARY **1996**, PAGE 151

Astron. Astrophys. Suppl. Ser. **115,** 151-159 (1996)

Atomic data from the IRON Project. XI. The $^2P^\circ_{\frac{1}{2}} - {}^2P^\circ_{\frac{3}{2}}$ fine-structure lines of Ar VI, K VII and Ca VIII

H.E. Saraph and P.J. Storey

Department of Physics and Astronomy, University College London, London WC1E 6BT, UK

Received February 27; accepted June 21, 1995

Abstract. — We give collision strengths and collision rates for electron excitation of the $^2P^\circ_{\frac{1}{2}} - {}^2P^\circ_{\frac{3}{2}}$ fine-structure transitions in the aluminium-like ions Ar VI, K VII and Ca VIII, at 4.53, 3.19 and 2.32μ respectively. The ground configuration of ions in the aluminium sequence has three electrons in the M-shell. Electron correlation effects are very strong in these ions because the subshells are energetically very close. They manifest themselves in large resonance structures that dominate the collision strengths. The accuracy of calculated collision rates depends critically on the accuracy with which the positions and shapes of these resonances are determined. This paper is a first attempt to provide collision rates for aluminium sequence ions that have been calculated taking full account of these electron correlation effects.

Key words: atomic data — atomic processes

1. Introduction

The IRON Project (Hummer et al. 1993) is an international collaboration that coordinates human resources so as to maximise the production of reliable electron collision data for ions of astrophysical interest. The first goal of the IRON Project was to calculate cross-sections and rate coefficients for electron impact excitation of ground term fine-structure transitions for abundant elements. In the case of the higher members of the aluminium sequence the only data available for most ions are the calculations by Krüger & Czyzak (1970) and by Blaha (1968). These were made using single configuration target ions described by LS - coupling. The scattering process was described in the distorted wave approximation and hence no resonance structure could be obtained. The present paper describes a coupled channel calculation that includes both resonance effects and the relativistic mass and Darwin terms of the Breit Pauli operator explicitly. Our aim is to calculate the thermally averaged collision strength for the $^2P^\circ_{\frac{1}{2}} - {}^2P^\circ_{\frac{3}{2}}$ ground state fine-structure transition at the temperatures appropriate to photoionized plasmas, up to about 20000 K. We are therefore primarily concerned to obtain accurate collision strengths within about one Rydberg of threshold.

Like boron, aluminium has a p-electron outside a closed s-shell. The difficulties that were encountered in past attempts to calculate reliable collision data for boron - like ions (Blum & Pradhan 1992) can be expected to increase significantly for aluminium - like ions because of the associated d-shell and the small energy gap between the M– and the N–shells. We find that for the three ions with nuclear charge Z=18 to 20 up to twenty target terms are necessary in order to include all the possible resonances that can occur in the low energy region. These calculations are described in Sect. 2. The calculation of the collision data is described in Sect. 3, and the results are presented and discussed in Sect. 4. Relativistic effects have been treated in an approximate way and this aspect is discussed in Sect. 5. We refer readers to the paper by Hummer et al. (1993) for details of the theory, numerical methods and a description of the computer programs. All energies are given in Rydberg units.

Send offprint requests to: P.J. Storey

2. Target representations

A schematic diagram of the term structure of Ar VI is shown in Fig. 1. The lowest terms belong to configurations of the $n = 3$ complex, and a few terms of configurations including $n = 4$ orbitals are present at higher energies. The picture is broadly similar for K VII and Ca VIII. Resonances in the electron scattering cross-section are due to quasi-bound states of the Si-like ion which form Rydberg series converging on the states of the Al-like ion. Our target for the scattering calculation should include sufficient

terms so that all resonances that can appear in the near threshold region are represented in the total wavefunction. The energies of the lowest members of the Rydberg series can be estimated by adding the energy of a valence electron to that of a parent term of the Al-like ion. The energy E of a valence electron state relative to the parent term is related to its effective quantum number, ν by

$$E = -\frac{z^2}{\nu^2}, \quad (1)$$

where z is the residual charge on the ion. The wavefunction for the scattering problem contains a component which is composed solely of target orbitals. Since our target contains all electron configurations of the n=3 complex as well as some configurations involving 4s and 4p orbitals, all scattering resonances arising from the n=3 complex of the Si-like ion and all low-lying resonances involving 4s and 4p orbitals are represented in the total scattering wavefunction. The lowest resonances which are omitted will be those involving a target state and a 4d orbital. For the three ions studied here one obtains, using a typical value of $\nu(4d) = 3.8$

$$1.7 \leq -E(4d) \leq 3.4 \text{ Ryd.} \quad (2)$$

If one is interested in low temperature collision rates it is necessary to calculate the collision strengths at energies from the excitation threshold to about 1 Ryd. The calculations must include and fully delineate all resonance structures. Using expression 2 one sees that all target terms with energies less than 2.7 Ryd must be included for Ar VI and all those with energies less than 4.4 Ryd for Ca VIII.

Table 1 lists the electron configurations used to expand the target wavefunctions. The configuration set was chosen to give the best agreement between calculated and experimental energies for the target states and also to minimize the difference between target oscillator strengths calculated in the length and velocity formulations. No non-physical orbitals were included in the target expansion. Such orbitals can improve the wavefunctions of low-lying target states, but also introduce spurious resonances in the scattering cross-section. The configuration list includes all configurations belonging to the n=3 complex. This ensures that all n=3 complex resonances are represented in the scattering calculation.

The target calculations were carried out in LS coupling but included the mass and Darwin terms of the Breit Pauli operator. These two relativistic terms lead to significant shifts in the energies of the electron configurations, but do not cause any breakdown of LS-coupling. Thus the main relativistic contribution to the term energies is incorporated, but the whole calculation, for the target and the scattering can be carried out in LS-coupling, with the consequent reduction in numbers of channels compared to a full Breit Pauli scattering calculation. An extended version of the program SUPERSTRUCTURE (Eissner et al. 1974; Nussbaumer & Storey 1978) was used for all target calculations.

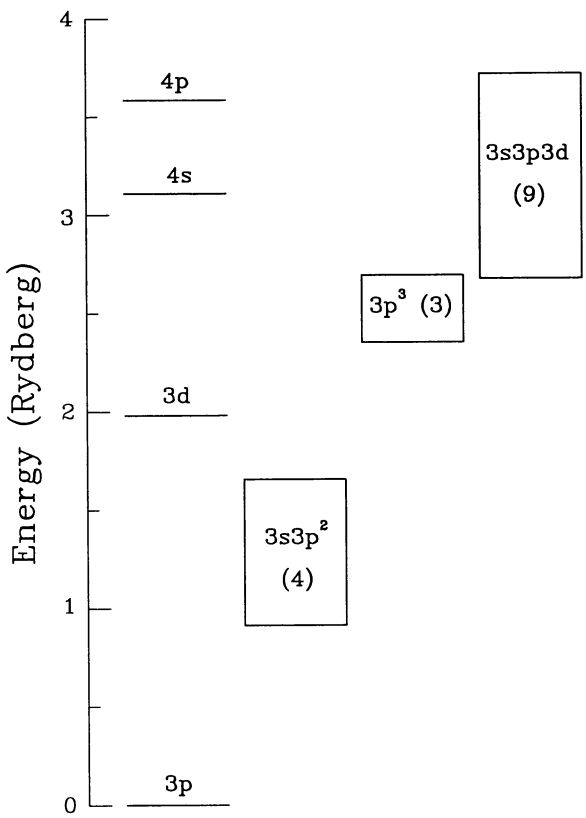

Fig. 1. Energy distribution of excited configurations of Ar VI

Tables 2 to 4 list the target terms and their calculated and experimental energies. For Ca VIII results obtained with the same configuration set but without any of the Breit Pauli terms are also listed. It is clear that relativistic effects cannot be neglected for these ions.

In Table 3 we give the results of a target structure calculation in which the spin-orbit and other fine-structure interactions are also included. For most terms, there is no significant difference in the centres of gravity when these additional interactions are included, as expected in the case where there are no fine-structure interactions between levels of different terms. Only in the case of the 3s3p3d ^{4}P°and ^{4}D°terms are the interactions between terms sufficiently large to affect the centres of gravity. From the point of view of term energies, it is therefore a good approximation to only include the mass and Darwin energy shifts.

The 'experimental' energies are those of the centres of gravity, relative to that of the ground term ^{2}P° and references are given in the tables. Thornbury et al. 1989 have studied the energies of terms $-3s^24s\,^2$S in the Al-sequence. Their values are used in all tables. By measuring the wavelengths of the ^{2}P°– ^{4}P intercombination lines, Träbert et al. (1988) have determined the uncertainties

Table 1. Ar VI, K VII and Ca VIII – target description

Closed shells: $1s^2 2s^2 2p^6$
CI for odd parity terms: $3s^2 3p$, $3p^3$, $3s3p3d$ and $3p3d^2$, $3s^2 4p$, $3s3p4s$, $3p3d4s$, $3s3p4d$, $3p^2 4p$, $3s4s4p$
CI for even parity terms: $3s3p^2$, $3s^2 3d$, $3s^2 4s$ and $3s3d^2$, $3d^3$, $3p^2 3d$, $3p^2 4s$, $3s3p4p$, $3s3d4s$, $3p3d4p$, $3s4s^2$, $3s4p^2$

Table 2. Target energies (in Rydberg) for Ar VI. $E_{\rm MD}$ calculated energies including mass and Darwin contributions, $E_{\rm exp}$ experimental energies Kelly 1987, for numbers in *italics* see text

config.	term	$E_{\rm MD}$	$E_{\rm exp}$
$3s^2 3p$	^{2}P^o	0.000	0.000
$3s3p^2$	^{4}P	0.890	0.911
...	^{2}D	1.198	1.194
...	^{2}S	1.569	1.534
...	^{2}P	1.694	1.655
$3s^2 3d$	^{2}D	2.044	1.979
$3p^3$	^{2}D^o	2.355	*2.350*
...	^{4}S^o	2.457	2.452
...	^{2}P^o	2.659	*2.674*
$3s3p3d$	^{4}F^o	2.695	*2.690*
...	^{4}P^o	2.892	2.907
...	^{4}D^o	2.924	2.939
...	^{2}D^o	3.027	*3.042*
$3s^2 4s$	^{2}S	3.119	3.106
$3s3p3d$	^{2}F^o	3.206	*3.221*
...	^{2}P^o	3.497	*3.512*
...	^{2}F^o	3.553	*3.568*
$3s^2 4p$	^{2}P^o	3.582	*3.582*
$3s3p3d$	^{2}P^o	3.680	*3.696*
...	^{2}D^o	3.699	*3.714*

Table 3. Target energies (in Rydberg) for K VII. $E_{\rm MD}$ calculated including mass and Darwin terms, $E_{\rm exp}$ experimental Levachov et al. 1990, $E_{\rm SS}$ calculated including contributions from the mass, Darwin and spin-orbit operators. For numbers in *italics* see text

config.	term	$E_{\rm MD}$	$E_{\rm exp}$	$E_{\rm SS}$
$3s^2 3p$	^{2}P^o	0.000	0.000	0.000
$3s3p^2$	^{4}P	1.023	1.044	1.023
...	^{2}D	1.372	1.366	1.373
...	^{2}S	1.777	1.740	1.776
...	^{2}P	1.915	1.875	1.916
$3s^2 3d$	^{2}D	2.336	2.266	2.336
$3p^3$	^{2}D^o	2.694	2.696	2.693
...	^{4}S^o	2.795	2.788	2.793
$3s3p3d$	^{4}F^o	3.054	*3.053*	3.053
$3p^3$	^{2}P^o	3.067	*3.053*	3.068
$3s3p3d$	^{4}P^o	3.315	3.291	3.323
...	^{4}D^o	3.349	3.321	3.343
...	^{2}D^o	3.455	3.410	3.455
...	^{2}F^o	3.664	3.587	3.664
$3s^2 4s$	^{2}S	4.000	3.984	4.000
$3s3p3d$	^{2}P^o	4.002	*3.985*	4.001
...	^{2}F^o	4.050	*3.996*	4.051
...	^{2}P^o	4.174	4.052	4.174
...	^{2}D^o	4.205	4.093	4.206

Table 4. Target Term energies (in Rydberg) for Ca VIII. $E_{\rm LS}$ calculated in pure LS-coupling. $E_{\rm MD}$ calculated including mass and Darwin contributions, $E_{\rm exp}$ experiment Redfors & Litzén 1989

config.	term	E_{LS}	$E_{\rm MD}$	$E_{\rm exp}$
$3s^2 3p$	^{2}P^o	0.000	0.000	0.000
$3s3p^2$	^{4}P	1.122	1.158	1.179
...	^{2}D	1.510	1.545	1.539
...	^{2}S	1.948	1.986	1.947
...	^{2}P	2.096	2.137	2.095
$3s^2 3d$	^{2}D	2.595	2.622	2.548
$3p^3$	^{2}D^o	2.964	3.034	3.037
...	^{4}S^o	3.058	3.135	3.126
...	^{2}P^o	3.366	3.439	3.411
$3s3p3d$	^{4}F^o	3.388	3.448	*3.419*
...	^{4}P^o	3.675	3.735	3.706
...	^{4}D^o	3.709	3.769	3.740
...	^{2}D^o	3.816	3.881	3.834
...	^{2}F^o	4.056	4.117	4.038
...	^{2}P^o	4.423	4.488	4.388
...	^{2}F^o	4.480	4.543	4.408
...	^{2}P^o	4.614	4.678	4.549
...	^{2}D^o	4.639	4.705	4.589
$3s^2 4s$	^{2}S	4.978	4.980	4.961

x that were attached to the earlier experimental energies for the quartets. The experimental term energies presented in the Tables have been corrected using these values for x where appropriate. For some of the target terms, experimental energies are not available. The energies of these terms were estimated by applying an empirical correction derived from the difference between experimental and calculated energies for other terms of the same configuration. These estimates are also included in the tables. In some instances the calculated target term energies were such that the terms were not in the same order as determined experimentally. In these cases energies were used that came as close as possible to the experimental ones without changing the order as originally calculated. Tables 2 to 4 list the energies used for the scattering calculation under the column heading $E_{\rm exp}$ and authors' estimates are distinguished by italic type.

3. The scattering calculation

The close-coupling method in the R-matrix formulation was employed, using the programs as developed for the IRON Project (Hummer et al. 1993). The mass and Darwin terms of the Breit Pauli operator were included explicitly. Calculated target energies were replaced by the experimental and estimated energies as listed in Tables

2 to 4, to ensure that resonance series limits are as accurately positioned as possible. The results of the scattering calculation were transformed algebraically to pair coupling and the spin-orbit interaction between the target terms was included as a perturbation by a second transformation that incorporated the so-called term coupling coefficients (Saraph 1978). In practice, at the low energies considered here the collision strengths are hardly affected by term coupling, and not at all at energies between the first and third target states. The fine-structure splitting of the target terms was neglected.

3.1. *Analysis of the near threshold collision strengths*

The collision strengths for K VII and Ar VI for the first 0.3 Ryd are shown in Figs. 2 and 3. In all three ions the energy range is covered by narrow resonances and also shows some broad areas of significantly enhanced background. Using formula (1) the number of resonances expected in a particular energy interval can be estimated. In Ar VI one can expect 32+ resonances between the excitation threshold and 0.1 Ryd. If one excludes usually weaker features of S and P symmetry, 17+ resonances should be seen. Most of these are concentrated between 0.05 and 0.1 Ryd and have configurations $3s3p^25d$ and $3s^23d4d$. One also expects one or two resonances of the configuration $3s3p3d^2$, although the energies of these states cannot be accurately predicted. Looking at Fig. 3 one can distinguish 15 peaks, which is in fair agreement with the rough estimate.

3.2. *The effect of target size*

Figure 4 shows the near-threshold collision strength for Ar VI when the highest 4 terms are omitted from the target expansion. The missing terms are $3s^24p\ ^2P^\circ$ and the highest three terms of the 3s3p3d configuration. The effect is that most resonances and the broad enhancement have shifted to higher energies.

The arguments of Sect. 2 suggest that all near threshold resonances are included in the calculation once the target size reaches 10 terms. Figure 4 shows that changing target size from 16 to 20 terms does not change the number of resonances in the near threshold region, but does significantly lower their energies. It is clear from Fig. 4 that the argument of Sect. 2 is too simplistic. There is a minimum target size necessary to ensure that all resonances are present, but the resonance energies will not be accurately calculated until all channels that contribute to the relevant wavefunction are explicitly included. The effect of varying the target size on collision rates is discussed in Sect. 4.1 below.

3.3. *Relativistic effects*

For Ca VIII a scattering calculation was also carried through without the mass and Darwin terms. A comparison of the near-threshold collision strengths, with and without those terms, is shown in Fig. 5. The positions of the near-threshold resonance features are seen to be sensitive to the relativistic effects, with shifts both up and down in energy. In our approximation, the mass and Darwin energy shifts are constant for a particular electron configuration. They also decline rapidly in magnitude as the orbital principal quantum number increases, so the largest shifts are expected for configurations in the $n = 3$ complex. The position of the broad feature in Fig. 5 is, however, hardly affected by the relativistic operators, indicating that it is not an $n = 3$ complex state, but rather formed from a core state plus a valence electron of relatively high principal quantum number. The effect of the mass and Darwin terms on collision rates is shown in Sect. 4.2 below.

3.4. *Calculated bound state energies*

In the absence of other calculations of collision data of similar sophistication in the literature, it is still possible to assess the accuracy of this calculation by examining bound state energies. Using the same target and scattering parameters, we have calculated energies for bound states of silicon - like Ca VII and the results are shown in Table 5.

Pradhan & Nahar (1993) have also calculated bound states for Ar V and Ca VII using the same program package. They had a smaller target with less configuration interaction than in the present work, but included non-physical orbitals to improve their target representation. They did not include the mass and Darwin relativistic terms. Average energy shifts due to the mass and Darwin terms are shown in Table 6 for several electron configurations of Ca VII. As expected the shifts are strongly configuration dependent and are largest for the $n = 3$ complex states.

Experimental energies are not available for members of Rydberg series with configurations $3s3p^2nl$ (other than $3s3p^3$), the higher members of which play an important role in determining the near-threshold collision strength. We can, however, estimate the expected error in their positions as follows. The average error in the calculated energies of the $3s3p^3$ terms is +0.030 Ryd, which corresponds to an error in the quantum defect for these terms of approximately 0.005. This would translate into an uncertainty in the calculated energy of a near threshold $3s3p^25p$ resonance of approximately 0.006 Ryd. As can be seen from Fig. 5, such uncertainties are comparable in magnitude to those arising from omission of the mass and Darwin terms.

Finally, we note that in the present *LS* calculations and in the work of Nahar & Pradhan (1993), the total energies of the lowest three terms of the $3s3p^3$ configuration lie below the experimental values. This problem is

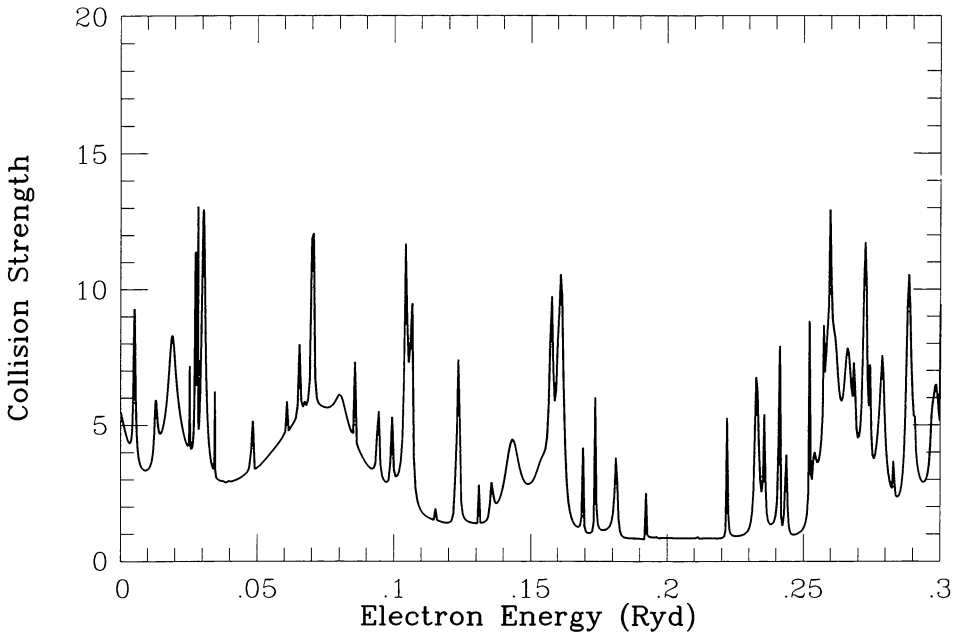

Fig. 2. Collision strengths for excitation of $(3s^2 3p)\ ^2P^\circ_{\frac{1}{2}} - {}^2P^\circ_{\frac{3}{2}}$ in K VII near the excitation thresholds

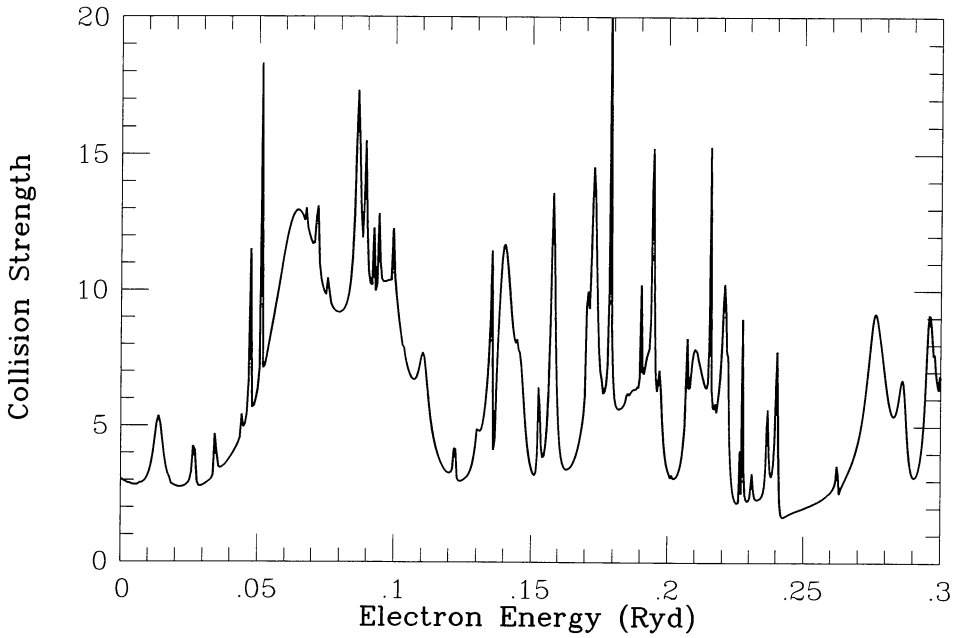

Fig. 3. Collision strengths for excitation of $(3s^2 3p)\ ^2P^\circ_{\frac{1}{2}} - {}^2P^\circ_{\frac{3}{2}}$ in Ar VI (20 target states) near the excitation thresholds

significantly reduced by the inclusion of the mass and Darwin terms.

4. Collision rates

The effective collision strength $\Upsilon(T)$ was obtained from the calculated collision strengths as described in Hummer et al. (1993). The collisional de-excitation rate coeffficient $q(T)$ is related to $\Upsilon(T)$ by

$$q = \frac{8.63\ 10^{-6}\Upsilon}{\omega T^{\frac{1}{2}}} \quad \mathrm{cm^3 s^{-1}},$$

where ω is the statistical weight of the upper state and T is the electron temperature in K. The energy for the collision strength calculation was such that adjacent points were separated by steps of 0.002 in effective quantum

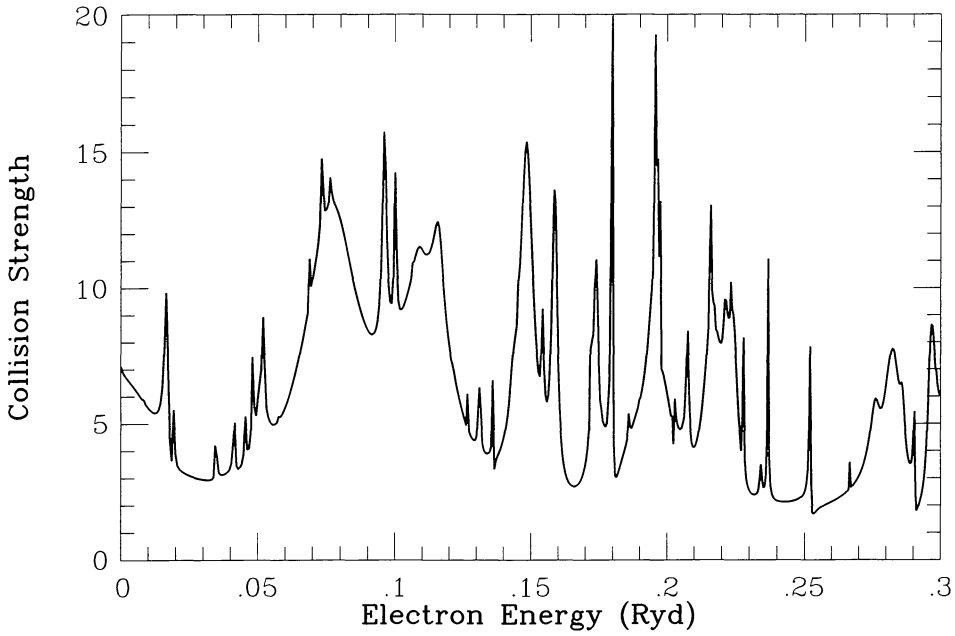

Fig. 4. Collision strengths for excitation of $(3s^2 3p)\ ^2P^\circ_{\frac{1}{2}} - {}^2P^\circ_{\frac{3}{2}}$ in Ar VI (16 target states) near the excitation thresholds

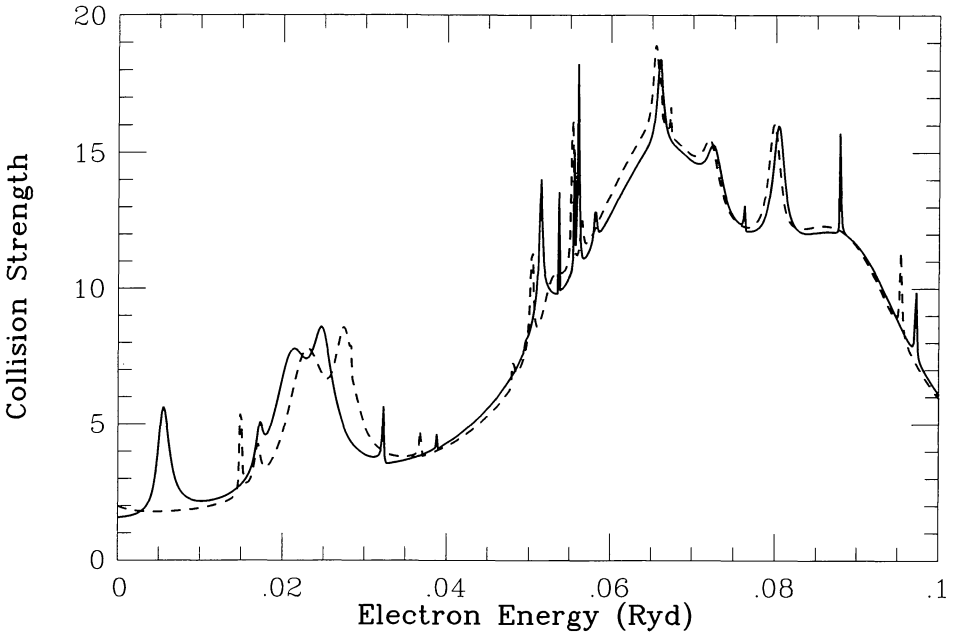

Fig. 5. Collision strengths for excitation of $(3s^2 3p)\ ^2P^\circ_{\frac{1}{2}} - {}^2P^\circ_{\frac{3}{2}}$ in Ca VIII. —— calculated with inclusion of mass and Darwin terms of the Breit Pauli operator. - - - pure LS coupling

number relative to the nearest target threshold. Very close to the excitation threshold, an interval of 0.0002 was used to accurately delineate narrow resonances. The method of obtaining the collision rate from the collision strengths involves linear interpolation between adjacent energies, followed by analytic integration over the electron velocity distribution in that energy interval (Hummer et al. 1993). The numerical accuracy of the collision rate calculation then depends only on the accuracy with which the collision strength can be linearly interpolated from the values at the mesh points. This procedure is accurate for arbitrarily low electron temperatures, which is not the case for a trapezoidal rule integration.

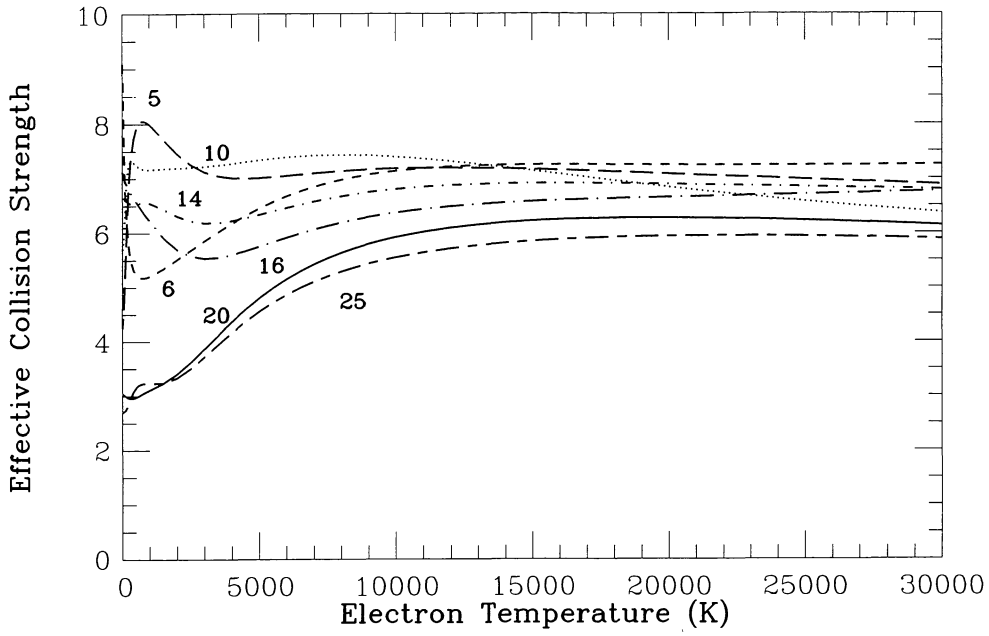

Fig. 6. Effective collision strengths for Ar VI as a function of the number of target terms

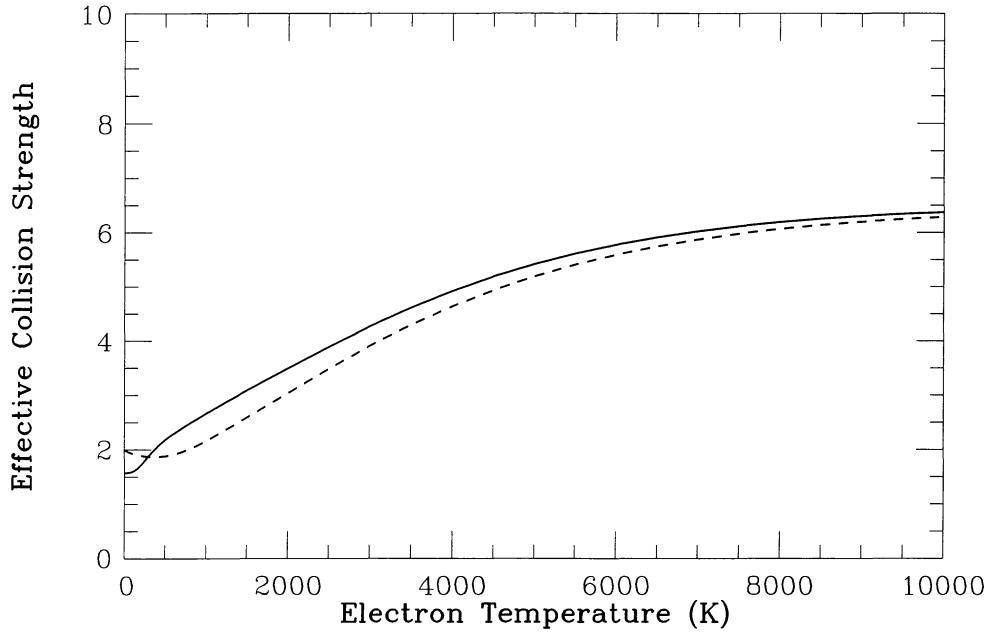

Fig. 7. Effective collision strengths for excitation of $(3s^2 3p)\ ^2P^\circ_{\frac{1}{2}} - {}^2P^\circ_{\frac{3}{2}}$ in Ca VIII. — calculated with inclusion of mass and Darwin terms of the Breit Pauli operator. - - - pure *LS* coupling

4.1. *Convergence of the close-coupling expansion*

To test the arguments given in Sect. 2 concerning minimum target size, we have calculated collision strengths near threshold for Ar VI for targets of 6, 10, 14, 16, 20 and 25 terms. The resulting collision rates are shown in Fig. 6. As discussed in Sect. 3.2 above, increasing the target size to more than 10 terms should not change the number of near threshold resonances, but does lower their energies. As a result, the low temperature collision rates are sensitive to target size, as some resonances move below threshold and others move down into the near threshold region. The effect on the collision rate of increasing the target size is unpredictable; there is no systematic trend. The effects are, naturally, greatest at the lowest

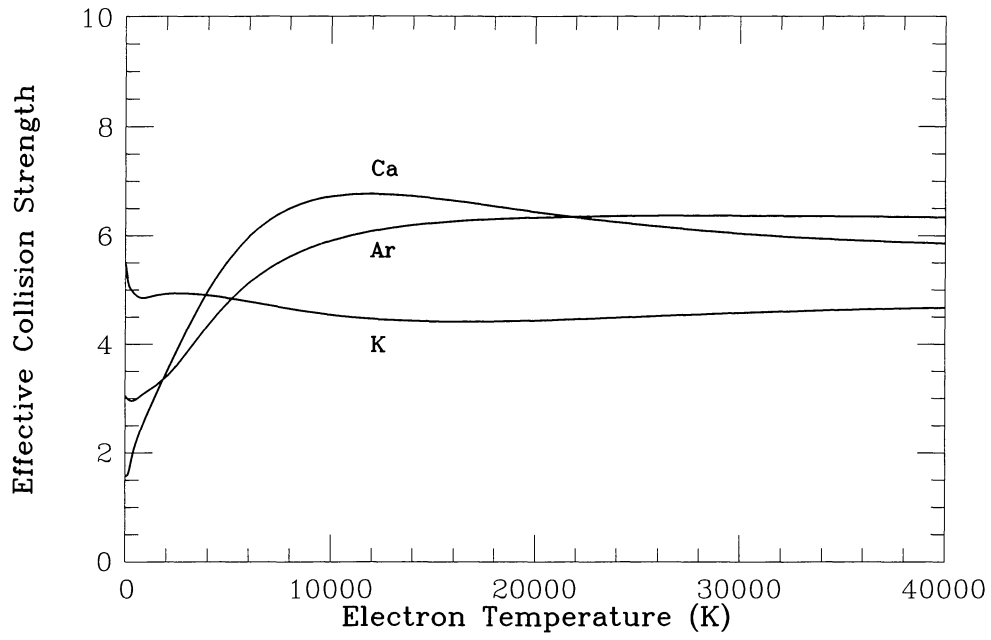

Fig. 8. Effective collision strengths for Ar VI, K VII and Ca VIII

Table 5. Ca VII: calculated (R-matrix method) and experimental term energies in Rydberg. MD, *LS* this paper with and without mass and Darwin terms, OP Nahar & Pradhan 1993 (opacity project), $E_{\rm exp}$ experiment Sugar & Corliss 1985

config	term	E_{LS}	$E_{\rm MD}$	$E_{\rm exp}$	$E_{\rm OP}$
$3s^23p^2$	^{3}P	-9.345	-9.358	-9.350	-9.364
...	...	0.000	0.000	0.000	0.000
...	^{1}D	0.177	0.177	0.174	0.177
...	^{1}S	0.437	0.438	0.421	0.437
$3s3p^3$	^{3}D°	1.401	1.435	1.436	1.402
...	^{3}P°	1.647	1.681	1.664	1.646
...	^{1}D°	1.813	1.843	1.830	1.819
...	^{3}S°	2.240	2.279	2.209	2.241
...	^{1}P°	2.293	2.328	2.275	2.301
$3s^23p3d$	^{3}P°	2.608	2.632	2.591	2.626
...	^{3}D°	2.687	2.711	2.670	2.704
...	^{1}F°	2.962	2.984	2.935	2.981
...	^{1}P°	3.055	3.079	3.014	3.061
$3s^23p4s$	^{3}P°	4.475	4.472	4.464	4.526
...	^{1}P°	4.526	4.524	4.519	4.585
$3s3p^24p$	^{5}S°	6.172	6.375	...	6.453
$3s3p3d^2$	^{5}S°	6.375	6.447	...	6.376
$3p^34s$	^{5}S°	7.563	7.634	...	7.609

Table 6. Typical changes in ionization energies for various configurations of Ca VII on inclusion of mass and Darwin terms, R-matrix calculations. All energies are in Rydberg

config.	shift	config.	shift	config.	shift
$3s^23p3d$	.020	$3s3p^3$	.035	$3s3d^3$	.090
$3s^23p4d$	.015	$3s3p^24p$	.044	$3p^33d$	.085
$3s^23d^2$	.040	$3s3p^25p$	.012	$3s3p3d4p$	.095
$3s^23d4d$	.018	$3s3p^23d$	.056	$3s3d^3$	.090
$3s^23p4f$	.015	$3s3p^24d$	.018	$3p^23d^2$	.115

temperatures. There is evidence from Fig. 6 that the collision rates are converging for 20 and 25 target terms, but the large spread in the low temperature ($T < 5000$ K) rates indicates that these should be treated with caution. All final results presented in this paper are obtained by cutting off the close-coupling expansion at 20 terms.

4.2. *Change of collision rate due to neglect of mass and Darwin terms*

The effect of the mass and Darwin relativistic terms on the Ca VIII collision rate is shown in Fig. 7. The low temperature region is particularly sensitive, whilst at high temperatures the effect is almost negligible. The low temperature effect depends on the positions of resonances due to core states and will vary greatly for individual ions.

5. Conclusion

Our final results for the effective collision strengths are given in Table 7 and Fig. 8. For Ar VI we give those obtained with the 20-state target, to maintain consistency with the other ions. As discussed above, the results are sensitive to target size, particularly for low temperatures. Based on the tests carried out for Ar VI, we consider that our target expansions are sufficiently large to have ensured convergence to within ten percent at the higher temperatures ($T > 5000$ K). At lower temperatures the uncertainty in the calculated effective collision strengths may well be significantly greater.

We have included relativistic effects through the mass and Darwin energy shifts, and via term coupling

Table 7. Effective collision strengths for Ar VI, K VII and Ca VIII

T(K)	Υ(Ar VI)	Υ(K VII)	Υ(Ca VIII)
0	3.05	5.47	1.56
20	3.04	5.42	1.57
50	3.02	5.33	1.57
100	3.00	5.20	1.59
200	2.97	5.05	1.71
300	2.95	4.99	1.89
400	2.96	4.95	2.05
500	2.97	4.91	2.17
600	3.00	4.88	2.28
700	3.03	4.86	2.38
800	3.06	4.85	2.48
900	3.08	4.85	2.57
1000	3.11	4.85	2.66
1500	3.23	4.90	3.08
2000	3.40	4.93	3.49
2500	3.62	4.93	3.89
3000	3.86	4.93	4.28
3500	4.11	4.92	4.65
4000	4.35	4.90	4.98
4500	4.57	4.87	5.29
5000	4.78	4.85	5.55
5500	4.96	4.81	5.78
6000	5.13	4.78	5.98
6500	5.27	4.75	6.15
7000	5.40	4.71	6.29
7500	5.51	4.68	6.40
8000	5.61	4.65	6.50
8500	5.70	4.62	6.58
9000	5.77	4.59	6.64
9500	5.84	4.56	6.68
10000	5.90	4.53	6.72
11000	6.00	4.49	6.75
12000	6.08	4.46	6.76
13000	6.14	4.44	6.75
14000	6.19	4.42	6.72
15000	6.23	4.41	6.68
16000	6.26	4.41	6.64
18000	6.30	4.41	6.53
20000	6.33	4.43	6.43
24000	6.36	4.49	6.24
28000	6.36	4.54	6.09
32000	6.36	4.60	5.98
36000	6.35	4.64	5.90
40000	6.33	4.67	5.86

coefficients, which allow for fine-structure interactions in the target. This method does not, however, permit us to allow for the change in threshold energy caused by the fine-structure splitting of the ground term. These splittings are 0.020, 0.029 and 0.039 Ryd for Ar VI, K VII and Ca VIII respectively. In our approximation, the threshold for excitation of the $^2P^\circ_{\frac{1}{2}} - {}^2P^\circ_{\frac{3}{2}}$ transition occurs at an energy corresponding to the centre of gravity of these two levels, rather than at the energy of the $^2P^\circ_{\frac{3}{2}}$ level itself. Thus the resonances that occupy the energy range from threshold to one third of the fine-structure splitting may not be relevant for the calculation of the collision rate, although a full treatment of relativistic effects would have to be made to be sure. The energy ranges involved are, however, small and lead to uncertainties in the collision rates at very low temperatures, where there are also large uncertainties due to other factors.

Acknowledgements. The authors wish to acknowledge the support of the SERC/PPARC through grant GR/H94979.

References

Blaha M., 1968, Ann. Astrophys. 31, 311
Blum R.D., Pradhan A.K., 1992, ApJS 80, 425
Eissner W., Jones M., Nussbaumer H., 1974, Comput. Phys. Commun. 8, 270
Hummer D.G., Berrington K.A., Eissner W., et al., 1993, A&A279, 298
Kelly R.L., 1987, J. Phys. Chem. Ref. Data 16, Suppl. 2
Krüger T.K., Czyzak S.J., 1970, Proc. R. Soc. London Ser. A 318, 531
Levashov V.E., Ryabtsev A.N., Churilov S.S., 1990, Opt. Spectrosc. 69, 20
Nussbaumer H., Storey P.J., 1978, A&A64, 139
Pradhan A.K., Nahar S.N., 1993, J. Phys. B: At. Mol. Opt. Phys. 26, 1109
Redfors A., Litzén U., 1989, J. Opt Soc. Am. B 8, 1447
Saraph H.E., 1978, Comput. Phys. Commun. 15, 247
Sugar J., Corliss C., 1985, J. Phys. Chem. Ref. Data 14, Suppl. 2
Thornbury J.F., Hibbert A., Träbert E., 1989, Phys. Scr. 40, 472
Träbert E., Heckmann P.H., Hutton R., Martinson I., 1988, J. Opt. Soc. Am. B 5, 2173